PHYSICAL REVIEW VOLUME 181, NUMBER 3 15 MAY 1969

First-Order Raman Effect in Wurtzite-Type Crystals

C. A. Arguello,* D. L. Rousseau, and S. P. S. Porto
Departments of Physics and Electrical Engineering, University of Southern California, Los Angeles, California 90007

(Received 5 December 1968)

First-order Raman scattering from BeO, ZnO, ZnS, and CdS, all having the wurtzite structure (C_{6v}), has been investigated. A discussion of the effects of the competition between the long-range electrostatic forces and the short-range forces due to anisotropy in the interatomic force constants on the vibrational spectrum has been included. A series of scattering diagrams are presented showing the geometrical arrangements necessary to observe all the $k=0$ phonons for this type of crystal structure. In BeO the E_2 mode was resolved from the transverse modes for the first time. The assignments of the E_2 modes in ZnS differ from previous investigations. From absolute intensity measurements, electro-optic coefficients for BeO, ZnO, and CdS were determined.

INTRODUCTION

Crystals with the wurtzite symmetry form an important class of semiconductors, which has been intensively studied for several years.[1–3] The innumerable investigations made on these crystals have utilized nearly every available experimental and theoretical technique. The relative simplicity of the wurtzite structure, the large number of materials having this symmetry, and the existence of the very closely related group of materials with the zinc-blende structure are the major factors which have made the investigation of these crystals very attractive.

Wurtzite crystals exhibit one of the simplest uniaxial structures and therefore form an important class of materials to analyze by Raman spectroscopy when fundamental physical processes are being investigated. Since wurtzite belongs to the space group $C_{6v}{}^4$ ($C6_3mc$) with two formula units per primitive cell and with all atoms occupying C_{3v} sites,[4] group theory predicts the following lattice phonons[5]: an A_1 branch in which the Raman-active phonon is polarized in the z direction and which is infrared active in the extraordinary ray; an E_1 branch in which the phonon polarized in the xy plane can be observed in the infrared in the ordinary ray spectrum, and which is also Raman active; two E_2 branches which are Raman active; and two silent B_1 modes. The nonvanishing components of the polarizability tensor are presented below for each mode, and for the polar phonons the direction of polarization is indicated in parentheses.

$$A_1(z)=\begin{bmatrix} a & 0 & 0 \\ 0 & a & 0 \\ 0 & 0 & b \end{bmatrix},$$

$$E_1(x)=\begin{bmatrix} 0 & 0 & c \\ 0 & 0 & 0 \\ c & 0 & 0 \end{bmatrix},$$

$$E_1(y)=\begin{bmatrix} 0 & 0 & 0 \\ 0 & 0 & c \\ 0 & c & 0 \end{bmatrix},$$

$$E_2=\begin{bmatrix} d & d & 0 \\ d & -d & 0 \\ 0 & 0 & 0 \end{bmatrix}.$$

Our objective in this paper is to discuss the Raman spectra of four crystals (BeO, ZnO, ZnS, CdS) with the wurtzite structure but to include a more detailed explanation of the polar phonons than has been presented in such papers in the past; and to show that these crystals clearly confirm the Poulet[6] and Loudon[7] formulations which predict frequency shifts and apparent group-theory selection rule breakdown for phonon propagation in directions other than along the crystallographic axes. In addition, we wish to carefully explain the wide variety of experimental arrangements which are necessary to use to properly observe all the phonons. Finally, absolute intensity measurements have been made on the longitudinal and transverse phonons for BeO, ZnO, and CdS, and from these values the electro-optic coefficients have been calculated.

THEORY

The frequency of an optical phonon which is infrared active is split into a longitudinal (LO) and a transverse (TO) component by the macroscopic electric field associated with the longitudinal phonon. This electric field serves to stiffen the force constant of the phonon and thereby raise the frequency of the LO over that of

---

* On leave from Department of Physics, University of Campinas, Brazil.

[1] D. C. Reynolds, C. W. Litton, and T. C. Collins, Phys. Status Solidi **9**, 645 (1965); **12**, 3 (1965).

[2] *Physics and Chemistry of II-VI Compounds*, edited by M. Aven and J. S. Prenner (Wiley-Interscience, Inc., New York, 1967).

[3] *II-VI Semiconducting Compounds, 1967 International Conference*, edited by D. G. Thomas (W. A. Benjamin, Inc., New York, 1967).

[4] W. L. Bragg, Phil. Mag. **39**, 647 (1920).

[5] D. L. Rousseau, R. P. Bauman, and S. P. S. Porto (to be published).

[6] H. Poulet, Ann. Phys. (Paris) **10**, 908 (1955).

[7] R. Loudon, Advan. Phys. **13**, 423 (1964).

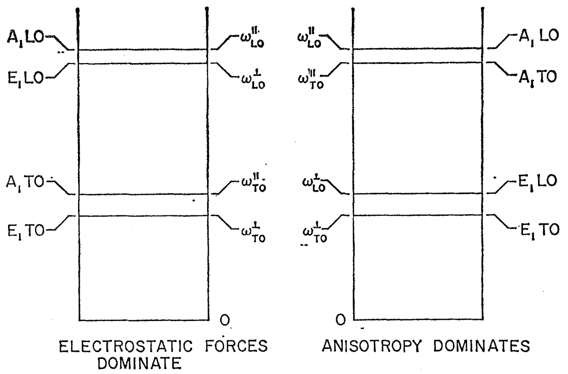

FIG. 1. Schematic energy-level diagrams for the two limiting cases. Left: Electrostatic forces predominate over the anisotropy in the interatomic forces. Right: Anisotropy forces predominate over electrostatic forces. The levels are appropriate for that region of the phonon dispersion curve near the zone center but out of the polariton region (i.e., $k\cong 10^5$ cm^{-1}). The relative values of the frequencies reflect a negative uniaxial crystal.

the TO. The consequences of this process on the static dielectric constant (ϵ_0) of the crystal are expressed by the well-known Lyddane-Sachs-Teller relationship[8]:

$$\epsilon_0=\epsilon_\infty(\omega_{LO}/\omega_{TO})^2, \tag{1}$$

where ω_{LO} and ω_{TO} are the frequencies of the longitudinal and transverse components, respectively, and ϵ_∞ is the high-frequency dielectric constant.

In simple cubic crystals such as zinc blende, this LO-TO splitting is very large and the first-order Raman spectrum consists of two phonons, one which is longitudinal and one which is transverse.

The situation is far more complicated in uniaxial crystals, though, as it becomes necessary to consider simultaneously two independent forces: the long-range electrostatic forces responsible for the longitudinal-transverse splitting, and the short-range interatomic forces, which exhibit the anisotropy of the force constants, and which require the phonons to follow group theoretical selection rules. It should be pointed out at this juncture that there have been several different notations used to specify the type of phonon under discussion for uniaxial crystals and some confusion has resulted.[9] The primary problem has been the use of parallel ($\parallel$) and perpendicular ($\perp$) notations which have been used to indicate both phonon propagation and phonon polarization. In the present discussion the notation used by Loudon[7] has been adopted in which $\parallel$ indicates a phonon that is polarized along the optic axis. This is necessarily an A_1 phonon in the wurtzite structure. Perpendicular ($\perp$) refers to a phonon polarized in the plane perpendicular to the optic axis and is therefore an E_1 phonon in wurtzite. The phonon propagation direction will be separately indicated when relevant.

TABLE I. Types of phonons possible for various polarizations and propagation directions.

		Phonon polarization		
		$x(E_1)$	$y(E_1)$	$z(A_1)$
Phonon Propagation	x	LO$^{\perp}$	TO$^{\perp}$	TO$^{\parallel}$
	y	TO$^{\perp}$	LO$^{\perp}$	TO$^{\parallel}$
	z	TO$^{\perp}$	TO$^{\perp}$	LO$^{\parallel}$

If the phonon propagation direction is along the x, y, or z axis (where the z axis coincides with the optic axis), only pure longitudinal and pure transverse phonons of well-defined symmetry character are observed in Raman scattering. Table I lists the various phonons that may be observed for each of the Cartesian propagation directions and each of the polarizations. We see from this table, for example, that if a phonon is propagating in the z direction one may observed three possible modes: a TO$^{\perp}$ mode polarized in the x direction (xz component of the polarizability tensor), another TO$^{\perp}$ mode polarized in the y direction (yz component of the polarizability tensor $\neq 0$), and finally an LO$^{\parallel}$ mode polarized in the z direction (xx component of the tensor, for instance). By symmetry the two TO$^{\perp}$ modes are degenerate.

An important feature of Table I is that complete separation may be made between the parallel and perpendicular phonons. Consequently, independent Lyddane-Sachs-Teller relationships may be written for the ordinary and extraordinary directions. We have for the ordinary direction

$$\epsilon_0^{\perp}=\epsilon_\infty^{\perp}(\omega_{LO}^{\perp}/\omega_{TO}^{\perp})^2, \tag{2a}$$

and for the extraordinary direction

$$\epsilon_0^{\parallel}=\epsilon_\infty^{\parallel}(\omega_{LO}^{\parallel}/\omega_{TO}^{\parallel})^2. \tag{2b}$$

When the propagation direction is not along one of the axes the situation becomes more complicated and careful consideration must be given to the competition between the effects due to the long range and the short-range forces. It is most convenient to divide uniaxial crystals into two categories[10]: case I, in which the electrostatic forces dominate over the anisotropy of the interatomic forces, and case II, in which the short-range interatomic forces are much greater than the electrostatic forces. Although it turns out that crystals with the wurtzite symmetry fall into the first category, in the ensuing discussion wurtzite will be used to illustrate both cases.

Case I. Since the electrostatic forces dominate over the anisotropy in the short-range forces, the LO-TO splitting must be greater than the A_1-E_1 splitting, i.e., $|\omega_{LO}^{\parallel}-\omega_{TO}^{\parallel}|$ and $|\omega_{LO}^{\perp}-\omega_{TO}^{\perp}|\gg|\omega_{LO}^{\parallel}-\omega_{LO}^{\perp}|$

---

[8] R. H. Lyddane, R. G. Sachs, and E. Teller, Phys. Rev. **59**, 673 (1941).

[9] See, for example, Ref. 7; see also J. F. Scott and S. P. S. Porto, Phys. Rev. **161**, 903 (1967).

[10] We adopt here the same classification as that in Ref. 7.

and $|\omega_{TO}^{\parallel}-\omega_{TO}^{\perp}|$. The relative energy levels for this situation for $k\gg0$ are illustrated in Fig. 1. The above inequality of the frequencies requires that regardless of the propagation direction the phonons under consideration will always be either purely transverse or purely longitudinal. To understand the consequences of this requirement it is best to discuss what happens to various phonons as the propagation direction is varied.

First, consider an E_1 phonon propagating in the xy plane and observed in the Raman effect through xz scattering, as shown in Fig. 2. When the propagation direction is along the x axis, only the longitudinal component may be seen since the xz tensor component corresponds to a phonon that is polarized in the x direction. At some angle θ, both the transverse and the longitudinal modes appear in the spectrum and their intensity may be found by resolving the transverse and longitudinal displacement vector directions into the x-polarization vector direction. Consequently, when the propagation is along y only the transverse phonon may be seen.

When the propagation direction is between the x and z axes a mixing between A_1 and E_1 modes may occur. This may be seen by consideration of Fig. 3, in which an A_1 phonon (electric polarization in the z direction) with a yy tensor component is illustrated. When the propagation direction is along the x axis, only the transverse component can be seen in the A_1 spectrum. Along the directions k_2 and k_3 the phonons are pure transverse and pure longitudinal; but they have a mixed A_1 and E_1 symmetry character since the polarization directions of the phonons are intermediate between the A_1 polarization direction z and the E_1 polarization direction x. The intensity of the A_1 component of each phonon may be found by determining the polarization vector component in the z direction. The frequencies, which are located between the pure A_1 and E_1 frequencies, may be given by[7]

$$\omega_{LO}^2=\omega_{A_1\,LO}^2\cos^2\theta+\omega_{E_1\,LO}^2\sin^2\theta \qquad (3a)$$

for the longitudinal mode and

$$\omega_{TO}^2=\omega_{E_1\,TO}^2\cos^2\theta+\omega_{A_1\,TO}^2\sin^2\theta \qquad (3b)$$

for the transverse phonon. When the propagation is along z only the longitudinal A_1 phonon may be observed in the Raman effect.

Similar arguments may be applied to the other phonons and to different propagation directions. One must only remember that these polar phonons will always be almost purely transverse or purely longitudinal, and are therefore often referred to as quasitransverse and quasilongitudinal phonons.

Case II. If the shoft-range forces dominate over the long-range forces, we may write the inequalities $|\omega_{LO}^{\parallel}-\omega_{LO}^{\perp}|$ and $|\omega_{TO}^{\parallel}-\omega_{TO}^{\perp}|\gg|\omega_{LO}^{\parallel}-\omega_{TO}^{\parallel}|$ and $|\omega_{LO}^{\perp}-\omega_{TO}^{\perp}|$. In other words, the splitting between the A_1 and E_1 symmetry modes will be much greater than the LO-TO frequency splitting. In Fig. 1 the energy levels for this case are contrasted to those of case I. We shall now consider the same two illustrative scattering situations.

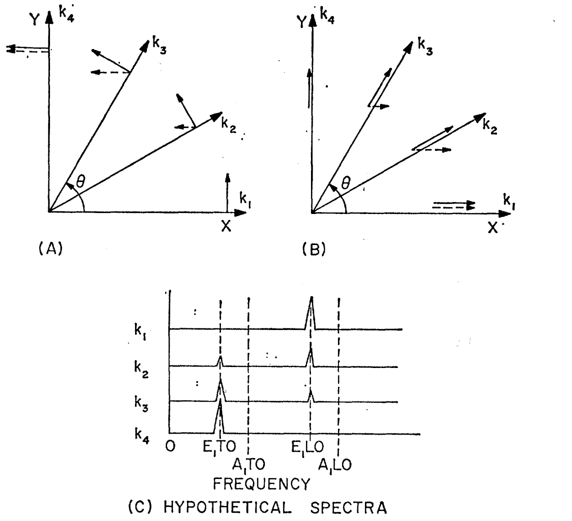

FIG. 2. E_1 phonon propagation in the xy plane when electrostatic forces dominate over anisotropy. (A) A transverse phonon is illustrated by the solid-line polarization vectors. The dashed lines correspond to the xz component (polarization in the x direction) of the polarizability tensor. (B) The longitudinal phonon is presented, and again the dashed line represents the xz component of the Raman tensor. (C) Hypothetical spectra of the xz tensor component are drawn for each of the propagation directions shown in (A) and (B).

Figure 4 depicts scattering from E_1 phonons which are being observed through the xz polarizability tensor

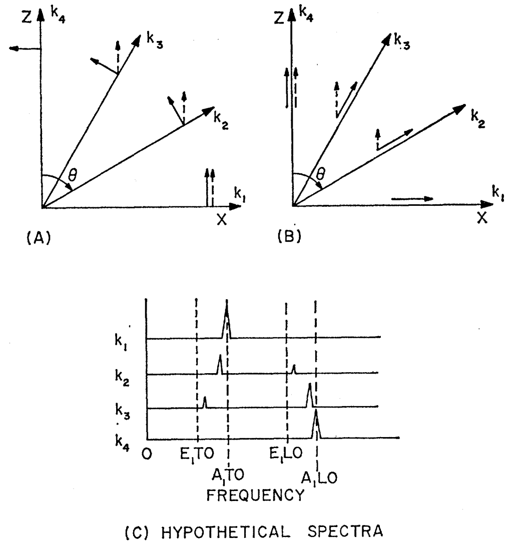

FIG. 3. Phonon propagation in the xz plane when electrostatic forces dominate over anisotropy. In the propagation directions k_1 through k_4, the solid vector represents the phonon polarization and the dashed vector the A_1 component of the phonon. (A) shows the transverse phonon and (B) the longitudinal. Hypothetical spectra are shown in (C).

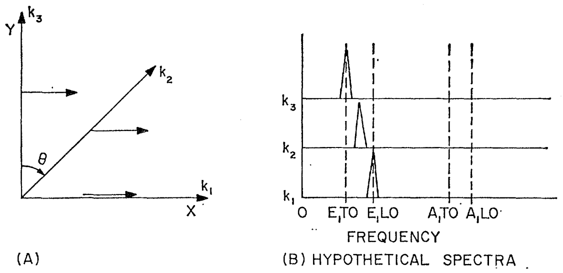

FIG. 4. E_1 phonon propagating in the xy plane when anisotropy dominates over electrostatic forces. (A) shows the phonon propagation (k_1-k_3) and polarization directions. The corresponding hypothetical spectra are shown in (B).

component, and which are polarized in the x direction. When the phonon propagates in the x direction only the E_1 LO can be observed. In the direction k_2, however, since the strong interatomic forces require the polarization to be maintained in the x direction, a pure longitudinal (or transverse) mode no longer exists. The phonons are still nearly pure E_1 phonons (and therefore might properly be termed quasi-E_1 phonons) and their frequency is located between the pure longitudinal and pure transverse E_1 frequencies. The frequency of this "quasi" mode will be given by[7]

$$\omega^2=\omega_{E_1\,\mathrm{TO}}{}^2\cos^2\theta+\omega_{E_1\,\mathrm{LO}}{}^2\sin^2\theta. \tag{4a}$$

Finally, in Fig. 4, when the observed phonon is propagating in the y direction it will be purely transverse.

An A_1 phonon propagating in the xz plane may undergo a similar shift from a longitudinal to a transverse phonon. Consider, as shown in Fig. 5, an A_1 phonon (a yy tensor component, for example) propagating along the x axis. It must be polarized in the z direction and is therefore transverse. In the intermediate direction k_2, it is of mixed transverse and longitudinal character and its frequency may be given by[7]

$$\omega^2=\omega_{A_1\,\mathrm{TO}}{}^2\sin^2\theta+\omega_{A_1\,\mathrm{LO}}{}^2\cos^2\theta. \tag{4b}$$

When the propagation direction is along z only the pure longitudinal frequency may be seen in the A_1 spectrum. To determine which phonons will appear in other spectra it is only necessary to remember that when Eqs. (4a) and (4b) hold the polarization direction of the phonon will always be fixed and will be that predicted by the group-theoretical selection rules for the tensor component under consideration.

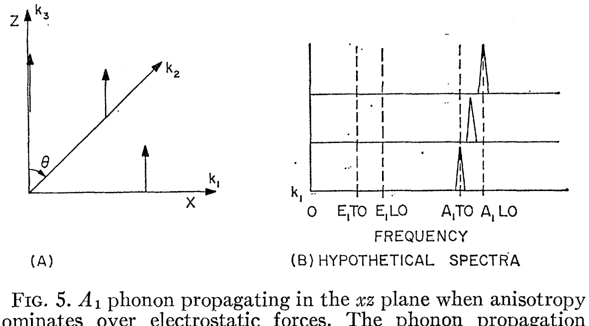

FIG. 5. A_1 phonon propagating in the xz plane when anisotropy dominates over electrostatic forces. The phonon propagation (k_1-k_3) and polarization directions are shown in (A) and hypothetical spectra are presented in (B).

As was first shown by Poulet[6] and later discussed in detail by Loudon,[7,11] the additional electron-lattice interaction caused by the macroscopic electric field carried by the longitudinal phonons greatly effects the scattering efficiencies. By using a perturbation method Loudon derived expressions for the transverse and longitudinal scattering efficiencies and found that the scattering intensity from a transverse phonon could be treated entirely by a deformation potential interaction. Scattering intensity from longitudinal phonons results from a deformation potential term and a term proportional to the electro-optic coefficient. For the zinc-blende structure with unpolarized incident light and unanalyzed scattered light, Loudon derived for the transverse and for the longitudinal scattering intensities the following relationships:

$$S_{\mathrm{TO}}=\frac{e^4V(n_t+1)L\Omega}{2\hbar^3m^4d^2Mc^4\omega_t}|R_{xy}{}^z|^2, \tag{5}$$

$$S_{\mathrm{LO}}=\frac{\hbar\omega_l(n_l+1)L\Omega}{4\pi c^4}\left|\frac{e^2}{\hbar^2\omega_l m^2 d}\left(\frac{\pi V}{M}\right)^{1/2}R_{xy}{}^z-\frac{\omega_i{}^2\epsilon_\infty{}^2}{2}\left(\frac{1}{\epsilon_\infty}-\frac{1}{\epsilon_0}\right)^{1/2}Z_{41}\right|^2, \tag{6}$$

where L is the scattering length over the solid angle Ω; V is the crystal volume and M is the reduced mass of the sublattices; ω_t, ω_l, and ω_i are the frequencies of the transverse phonon, the longitudinal phonon, and the incident light wave, respectively; d is the lattice constant; $R_{xy}{}^z$ is the deformation potential and is directly proportional to the polarizability derivative tensor; Z_{41} is the electro-optic coefficient; and $\hbar$, e, m, and c have their usual significance. (n_t+1) and (n_l+1) are the distribution functions for the transverse and longitudinal wave with

$$n=(e^{\hbar\omega/kT}-1)^{-1}. \tag{7}$$

These results, which are valid for cubic piezoelectric crystals, can be extended without difficulty to uniaxial crystals if we consider the Raman tensor $R_{\lambda\mu}{}^\kappa$ for phonons simultaneously Raman and infrared active (a $\lambda\mu$ tensor component with phonon polarization in the κ direction) as a third-order tensor symmetric in the last two indices ($R_{\kappa,\lambda\mu}=R_{\kappa,\mu\lambda}$). From the previously discussed selection rules for C_{6v} a third-order tensor of the form

$$\begin{bmatrix} \cdots & \cdots & \cdots & \cdots & c & \cdots \\ \cdots & \cdots & \cdots & c & \cdots & \cdots \\ a & a & b & \cdots & \cdots & \cdots \end{bmatrix}$$

is obtained which is identical to the general form of a

---

[11] R. Loudon, Proc. Roy. Soc. London **A275**, 218 (1963).

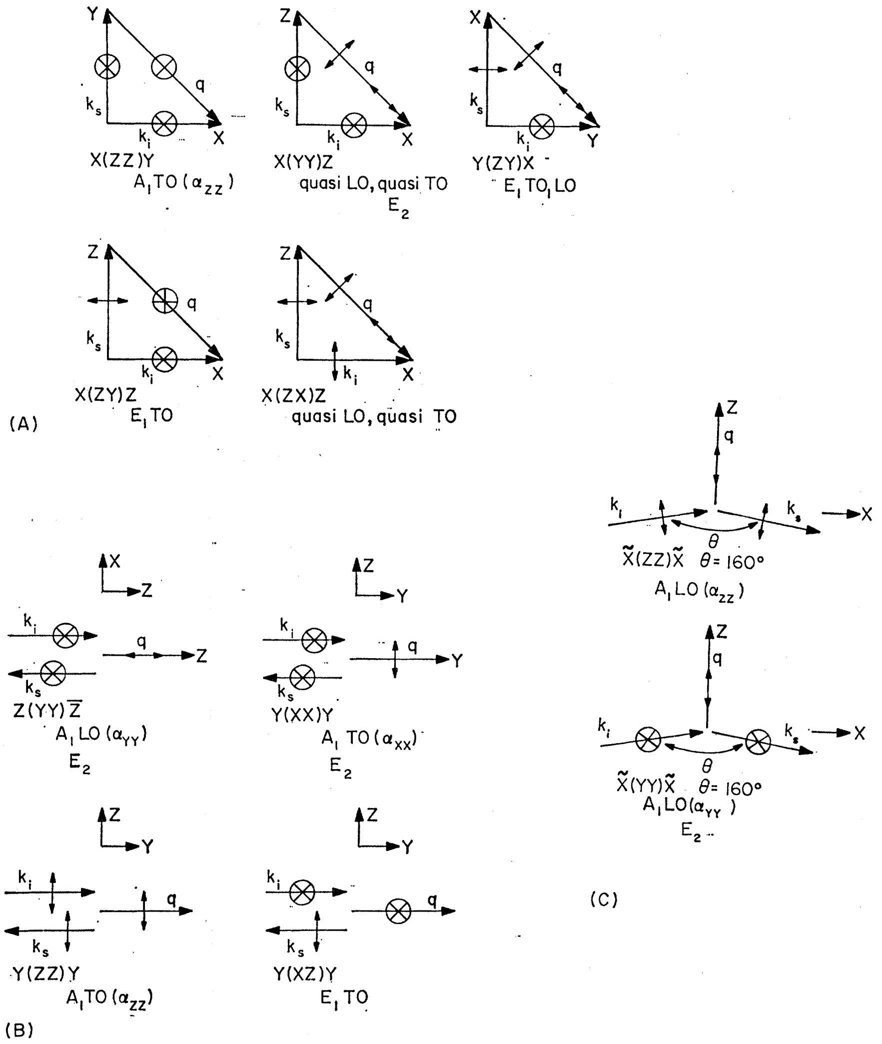

FIG. 6. Scattering diagrams for a variety of orientations when electrostatic forces dominate over anisotropy in a C_{6v} crystal. The directions of the incident and scattered photons are indicated by $\boldsymbol{k}_i$ and $\boldsymbol{k}_s$, respectively, and the phonon by q. The polarization directions are indicated by small arrows or by circled crosses, the latter indicating a direction perpendicular to the plane of the paper. The predicted phonons are listed below each diagram. Right angle, backward, and forward scattering are illustrated in (A), (B), and (C), respectively. It should be pointed out that the notations used to describe the forward scattering in (C) do not specify the propagation direction. This must be separatly indicated, but in this paper the geometry has been selected to always scatter from phonons propagating in the z direction.

third-order tensor describing the third-rank physical properties of a C_{6v} crystal.[12] Since the Raman tensor, then, has the same form as the electro-optic tensor, a one-to-one correspondence between their terms may be made. This result remains valid for any crystal symmetry. Combining Eqs. (5) and (6), an equation for the electro-optic coefficient may be derived, and for C_{6v} the three independent components Z_{13}, Z_{33}, and Z_{51} may be determined. The electro-optic coefficient measured in this way corresponds to one in which the frequency of the modulating electric field is that of the optical phonon and the refractive index change occurs at the frequency of the incident laser light.

EXPERIMENTAL

The Raman spectra were excited with a Spectra-Physics argon-ion laser emitting 1 W at 4880 and 5145 Å. The beam was focused on the sample with lenses of either 4 or 6.5 cm focal distances and the polarization was controlled with a quartz first-order half-wave plate. Light scattered from the crystals was gathered with an $f1.2$, 50-mm focal length lens and focused on the slits of a tandem Spex double spectrometer. The lens was positioned so as to match the $f6.8$ spectrometer optics, and the scattered light was analyzed by placing a polaroid sheet in front of the entrance slit. After the light was dispersed by the double monochromotor, the image of the exit slit was demagnified by a factor of 6,

---

[12] J. F. Nye, *Physical Properties of Crystals* (Oxford University Press, London, 1964), p. 124.

TABLE II. Fundamental optical modes of some wurtzite-type crystals (frequencies expressed in cm^{-1}).

Mode	BeO	ZnO	CdS (25°K)	ZnS (298°K)	ZnS (25°K)
E_2	338	101	43	55	...
E_2	684	444	256	724	280
A_1 (transverse)	678	380	234	274	280
Quasi-A_1 (transverse)	700	395	240	274	280
Quasi-E_1 (transverse)	702	398	239	274	280
E_1 (transverse)	722	413	243	274	280
A_1 (longitudinal)	1081	579	305	352	356
Quasi-A_1 (longitudinal)	1088	585	306	352	356
Quasi-E_1 (longitudinal)	1089	585	306	352	356
E_1 (longitudinal)	1097	591	307	352	356

and then carefully focussed on the photocathode to prevent spillover.

The crystals were cooled by boil-off helium gas and the temperature was monitored with a GaAs junction. All the crystals were cut such that the optical axis was perpendicular to two of the surfaces. The BeO crystal was obtained from S. B. Austerman of North American Aviation, Inc. The CdS was purchased from Clevite Corp.; the ZnO from Harshaw Chemical Co.; one ZnS crystal was purchased from Harshaw Chemical Co; and a second ZnS crystal was obtained from Professor G. F. J. Garlick.

All spectra discussed in this paper will be described by notations of the type[13] $x(zy)z$, where the directions inside the parentheses signify the polarizations of the incident and scattered beams, respectively. The letter preceding and following the parenthesis indicates the respective directions of the incident beam and scattered beams. In addition, back scattering may be indicated by $x(zy)\bar{x}$ and near-foward scattering (see subsequent discussion) by $\bar{x}(zy)\bar{x}$.

Rembering from the previous discussion that in wurtzite crystals electrostatic forces dominate over interatomic forces, experimental arrangements required to observe the various phonons may be specified. We illustrate the experimental arrangements by scattering diagrams in which the phonons appearing in each spectrum must conserve energy ($\nu=\nu_i-\nu_s$) and momentum ($\mathbf{q}=\mathbf{k}_i-\mathbf{k}_s$). In these diagrams the crystal optic axis is designated as the z axis.

Keeping in mind the Raman tensors and the associated polarizations previously discussed it may be readily determined which phonons may be seen in a large variety of orientations. These are indicated schematically for right angle scattering in Fig. 6(A). These scattering diagrams show the phonon propagation direction and the phonon polarization. The allowed phonons are also listed below each diagram. It is important to point out that in the $x(yy)z$ and $x(zx)z$ orientations in which the propagation direction is at 45° from both the x and the z axes, the scattering from the pure longitudinal and pure transverse phonons is of equally mixed symmetry character so that the polar phonon spectra in these two orientations are identical and the distinction between A_1 and E_1 is no longer valid. It should be noted that no pure A_1 LO phonons may be observed in right-angle scattering.[14]

To observe the pure LO phonons, back scattering and forward scattering have been used. The back-scattering diagrams are illustrated in Fig. 6(B) and the forward scattering in Fig. 6(C). In the back scattering only phonons of the well-defined character are observed and all the A_1 modes may be seen except the A_1 LO (α_{zz}), which must be seen by near forward scattering. In the forward scattering care must be taken that θ [see Fig. 6(C)] does not exceed about 160° or polaritons will be produced. In addition, when intensity calculations are made for the $\bar{x}(zz)\bar{x}$ orientation, it is necessary to make an angle correction as the polarization is not exactly along the z direction.

To make the absolute intensity measurements scattering from the 992-cm^{-1} line of benzene was used as a standard. The absolute Raman cross section of this line was measured by Damen, Leite, and Porto[15] with a 6328 Å laser source and more recently by Skinner and Nilsen's value of 1.05×10^{-29} cm^2/molecule sr cm^{-1} can readily be converted to a scattering efficiency of 0.27×10^{-6}/cm sr.

To obtain the absolute efficiencies the right-angle scattering from the E_2 modes of each of the three crystals ZnO, CdS, and BeO was measured and with all spectrometer and geometric settings the same, the scattering from the 992-cm^{-1} benzene line was measured. The E_2 intensities were then found by taking the ratios of their integrated areas to that of the benzene line. Corrections were made for the reflectivity of the crystal to both the incident and scattered light and for the different solid angles subtended by each crystal. The relative sensitivity of the spectrometer in both the horizontal and vertical polarizations was determined with a G.E. Model 6.6A/T4Q/1CL-200W quartz-iodine-tungsten lamp. By thereby establishing an E_2 mode as a secondary standard a variety of orientations could be used to obtain the desired LO and TO efficiencies without further resort to the benzene standard.

RESULTS AND DISCUSSION

A. Location and Assignment of Fundamentals

In Fig. 7, the Raman scattering spectra of BeO are shown. The frequencies of the fundamentals are designated in each spectrum, and this data have been compiled in Table II. The extra lines in the back-scatter-

---

[13] T. C. Damen, S. P. S. Porto, and B. Tell, Phys. Rev. **142**, 570 (1966).

[14] This is true only if the crystal is cut with its faces perpendicular to the crystallographic axes. However, if faces are cut such that they form 45° angles with both the x and z axes but contain the y axis, LO phonons propagating in the z direction may be observed. See Ref. 13.

[15] T. C. Damen, R. C. C. Leite, and S. P. S. Porto, Phys. Rev. Letters **14**, 9 (1965).

[16] J. G. Skinner and W. G. Nilsen, J. Opt. Soc. Am. **58**, 113 (1968).

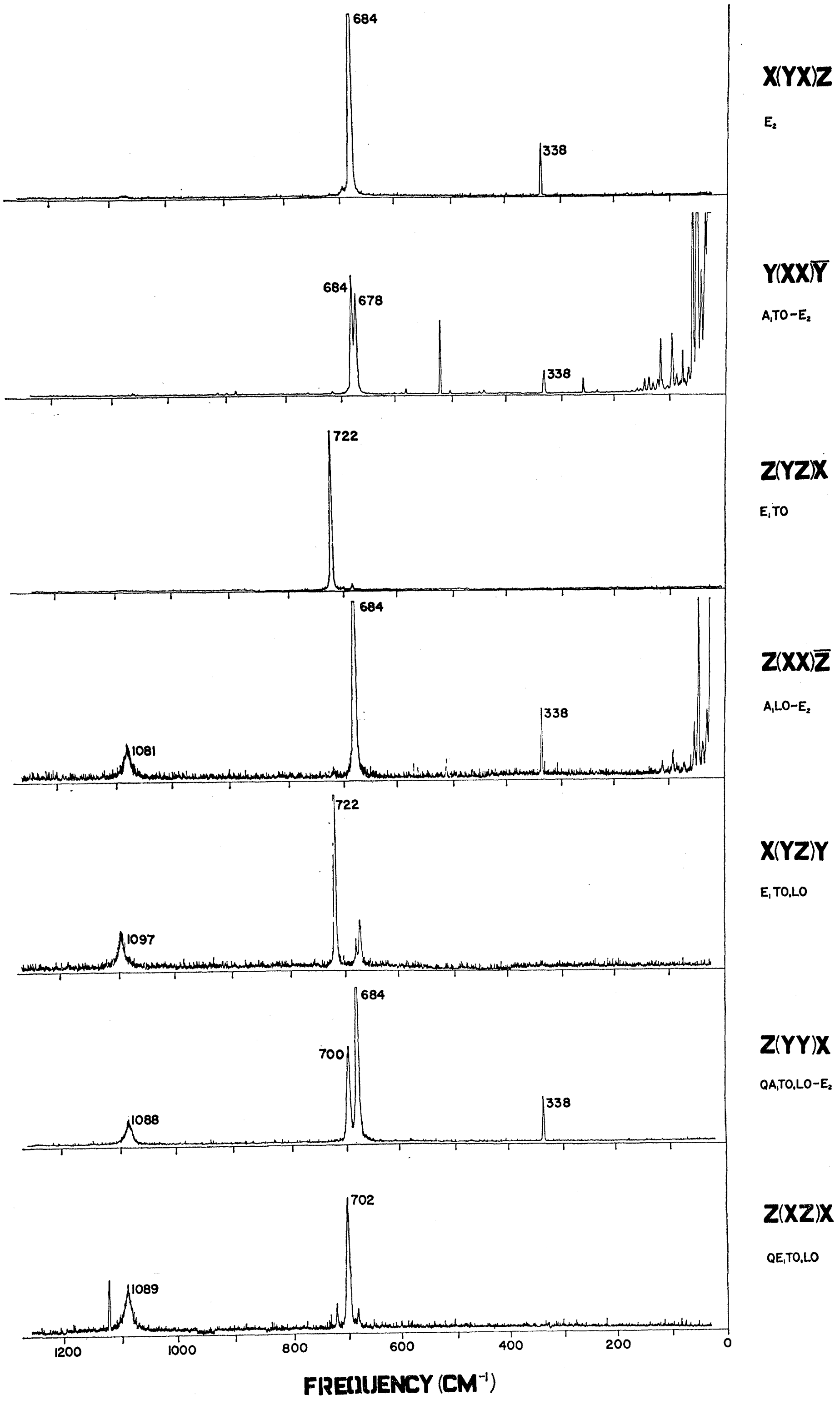

FIG. 7. Raman spectra of BeO. The "extra" lines in $y(xx)\bar{y}$ and $z(xx)\bar{z}$ are grating ghosts and argon fluorescence lines.

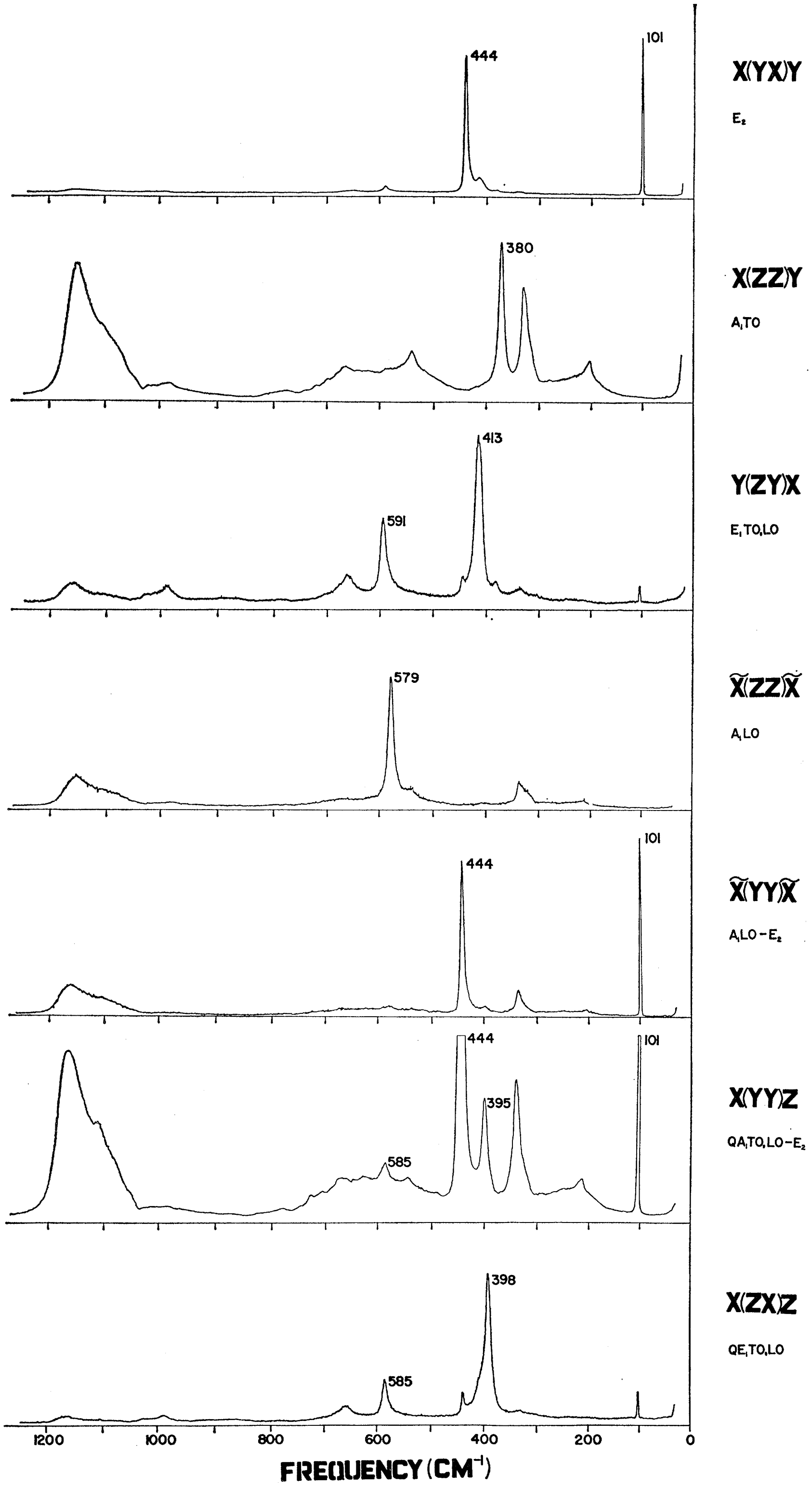

FIG. 8. Raman spectra of ZnO.

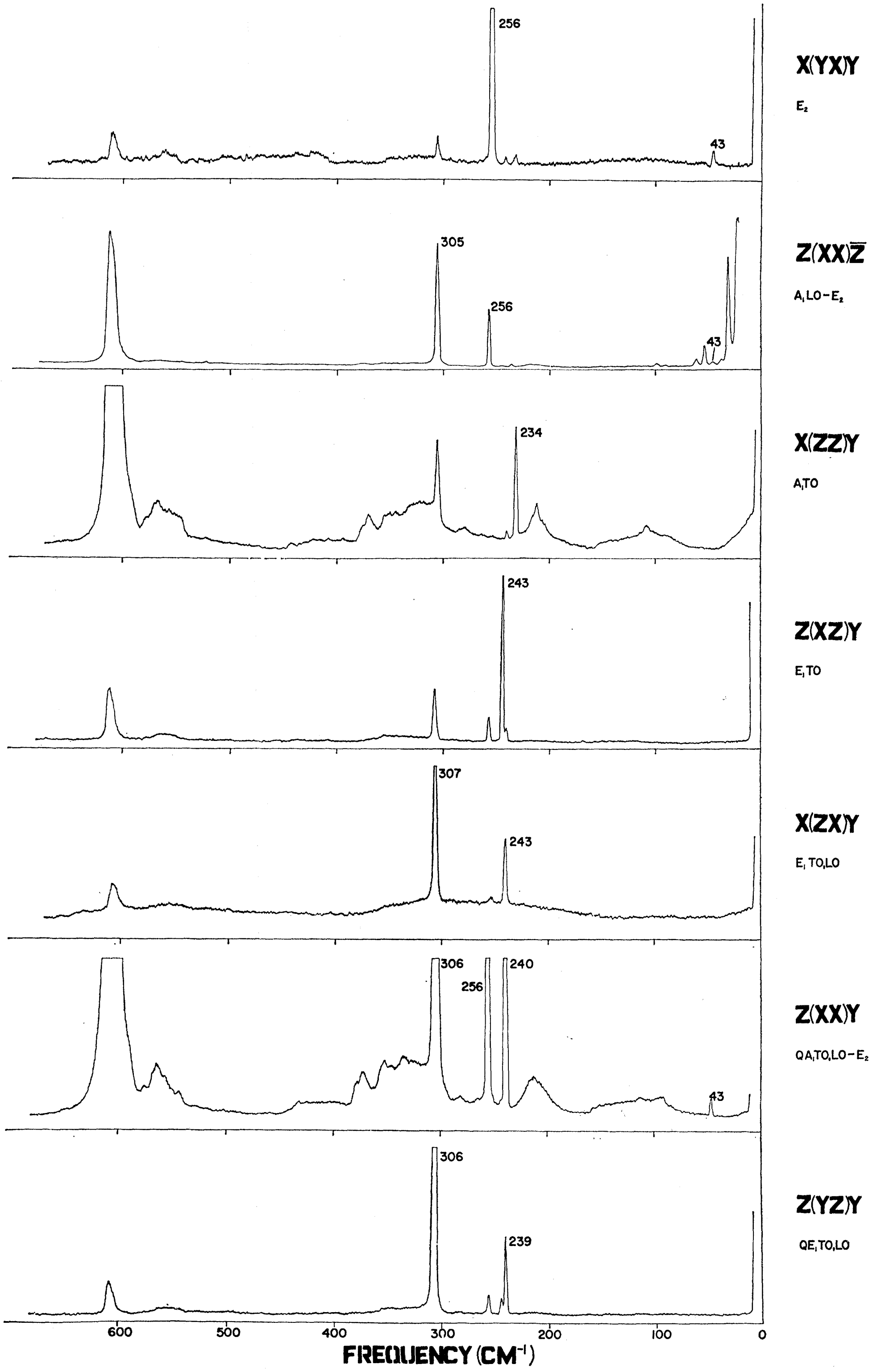

FIG. 9. Raman spectra of CdS at 25°K. The extra low-frequency lines result from grating ghosts.

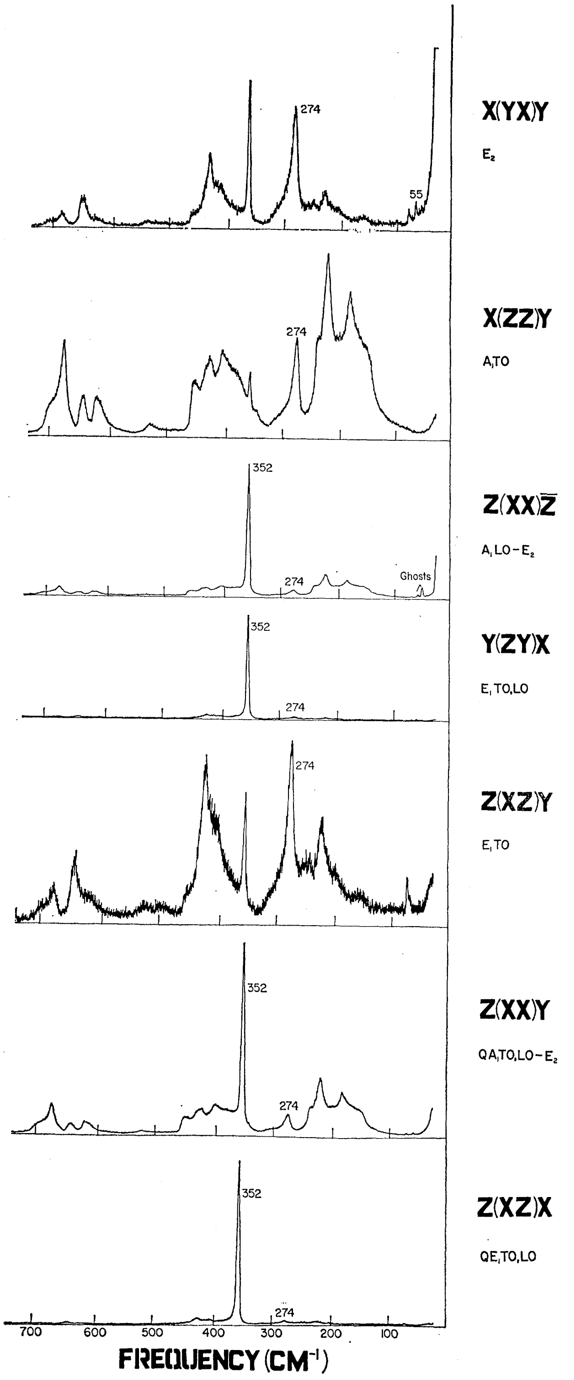

FIG. 10. Raman spectra of ZnS at 298°K.

ing spectra, $y(xx)\bar{y}$ and $z(xx)\bar{z}$, all were found to result from grating ghosts or from fluorescence from the argon laser. The assignments reported here agree with those previously reported[17] but we have been able to separate the high-frequency E_2 mode from the transverse mode, which could not be achieved in the prior investigation. In Fig. 7, the separation between the E_2 and the A_1 TO mode in the $y(xx)\bar{y}$ spectra and between the E_2 and the quasi-TO in the $z(yy)x$ spectrum is very clear. The depolarization ratios were all consistent with group-theoretical predictions, as can be seen by the spectra. The shifting of the longitudinal modes and the transverse modes in the $z(yy)x$ and $z(xz)x$ spectra are in excellent agreement with Loudon's predictions for a crystal in which electrostatic forces are much stronger than the forces due to anisotropy.

The ZnO spectra shown in Fig. 8 are in substantial agreement with those of Damen *et al.*[13] A point of considerable interest, however, is the difference in the intensity of the A_1 LO in the *yy* spectra and in the *zz* spectra. The prominence of the A_1 LO band at 579 cm^{-1} in the $\tilde{x}(zz)\tilde{x}$[18] spectrum is in marked contrast to its complete absence from the $\tilde{x}(yy)\tilde{x}$[18] spectrum. Such a difference can be accounted for by different values in the corresponding terms of the electro-optic coefficient. The intensity of this phonon in the quasilongitudinal A_1 spectrum $x(yy)z$ demonstrates the mixed character of the phonon, which has enabled it to share the E_1 LO intensity. The shift in frequency of both the LO and TO modes in the quasilongitudinal and quasitransverse mode spectra are again in exact agreement with the Loudon theory.

All the spectra of CdS were obtained at ~25°K, where the crystal is transparent to the 5145 Å incident laser beam, although at high laser power levels (~1 W) linear multiple photon absorption with subsequent fluorescence was observed. Analogous fluorescence was also seen in ZnS. In a previous investigation[19] of CdS, the low-frequency E_2 mode (at 43 cm^{-1} in this study) could not be observed clearly with 5145 Å excitation. Figure 9 shows that this mode is clearly present in our spectra and obeys the selection rules for an E_2 mode. [The extra lines in the $z(xx)\bar{z}$ spectrum are grating ghosts.] Our data also confirms the conclusions on the assignment of the modes made by Tell *et al.*[1], at higher temperatures. The frequency of the longitudinal and transverse modes vary as predicted in this crystal as in ZnO and BeO.

Recently, Brafman and Mitra[20] have reported on the Raman spectrum of ZnS. They found that the two E_2 modes were located at 72 and 286 cm^{-1}, the TO node of both A_1 and E_1 symmetry at 273 cm^{-1}, and the LO mode also of A_1 and E_1 symmetry was located at 351 cm^{-1}. From infrared data on mixed crystals, Lucovsky *et al.*[21] proposed that the E_2 modes are located at 48 and 287 cm^{-1}. Previously, Poulet, Klee, and Mathieu[22]

---

[17] E. Loh, Phys. Rev. **166**, 673 (1968).

[18] For these scattering geometries the phonon propagation is in the *z* direction. See Fig. 6(C).

[19] B. Tell, T. C. Damen, and S. P. S. Porto, Phys. Rev. **144**, 771 (1966).

[20] O. Brafman and S. S. Mitra, Phys. Rev. **171**, 931 (1968).

[21] G. Lucovsky, E. Lind, and E. A. Davis, in *II–VI Semiconducting Compounds, 1967 International Conference*, edited by D. G. Thomas (W. A. Benjamin, Inc., New York, 1967), pp. 1150–1163.

[22] H. Poulet, W. E. Klee, and J. P. Mathieu, in *Proceedings of the International Conference on Lattice Dynamics, Copenhagen, 1963* (Pergamon Press, Inc., New York, 1965), pp. 337–341.

had investigated the Raman scattering from ZnS and found the TO at 272 cm^{-1}, the LO at 349 cm^{-1}, and only one E_2 located at 217 cm^{-1}. Our assignments of the TO and LO modes are in agreement with both prior Raman investigations, as our spectra places the room-temperature TO frequency at 274 cm^{-1} and the LO at 352 cm^{-1}. (See Fig. 10.) We obtained identical spectra both with a crystal purchased from Harshaw Chemical Co. and with one grown in the laboratory of G. F. J. Garlick. By Laue x-ray analysis and by examination under a polarizing microscope it was determined that our crystals were predominatly of hexagonal character.

Our assignment of the two E_2 modes is at considerable variance with previous assignments. The line observed by Poulet *et al.* at 217 cm^{-1} and assigned as a E_2 was assigned by Nilsen,[23] who recently studied the two-phonon spectrum of hexagonal ZnS, as a second-order line resulting from the combination of two zone-edge longitudinal phonons. This is confirmed by our low-temperature spectra shown in Fig. 11 in which the line at 217 does not have the proper temperature dependence to be a one-phonon line. The intensity of a one-phonon line should have an $(n+1)$ temperature dependence while a combination should follow an $(n+1)^2$ temperature dependence, where n was defined by Eq. (7). In addition to the temperature dependence this line is found to be very prominent in the α_{zz} spectra, a further indication that it is not an E_2 mode. The line at 286 cm^{-1} is absent from all of our spectra as can be seen by Fig. 10. This suggests that its presence in the spectra of Brafman and Mitra may have resulted from inpurities in their crystal. Indeed, the spectra from both of our ZnS crystals agree very well with those of Nilsen obtained on crystals from different sources.

Brafman and Mitra observed the other E_2 mode at 72 cm^{-1}. We assumed that the line we have observed at 68 cm^{-1} is the same one and we studied its polarization characteristics. Although it was observed in the xx and xy spectra, Fig. 12 demonstrates that it was also seen in the xz spectrum with similar intensity. This represents a serious violation of the selection rules for an E_2 mode. In addition, its frequency just equals LO minus TO, which at the zone center should have the nonzero components xx, zz, xy, xz, in excellent agreement with our observations. (Its absence from the zz spectrum does not represent a selection-rule breakdown but only indicates that the intensity of this second-order line is weak for that component of the polarizability tensor.) As can be seen in Fig. 12, there is a mode at 55 cm^{-1} which satisfies the polarizability requirements for an E_2 mode. While this cannot unambiguously be assigned as an E_2 mode, its characteristics are strongly suggestive that this is in fact its origin. Other possibilities are that it is a second-order line from a zone point other than the edge or the center, or a local mode. These are both rather unlikely, so we have assigned the band at 55

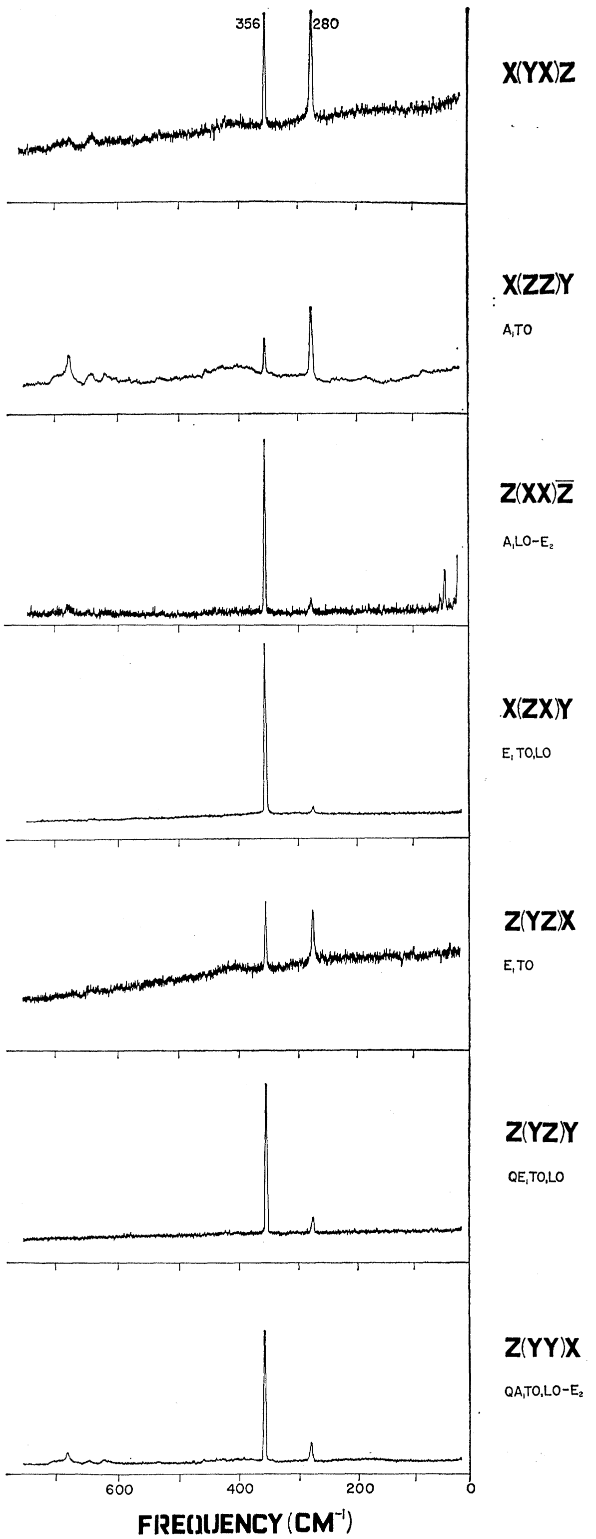

FIG. 11. Raman spectra of ZnS at 25°K.

---

[23] W. G. Nilsen (to be published).

TABLE III. Static dielectric constants obtained from Lydanne-Sachs-Teller (LST) relationship.[a]

	BeO		ZnO		CdS(25°K)		ZnS	
	LST	Literature	LST	Literature	LST	Literature	LST	Literature
$\epsilon_0^{\parallel}$	7.62	7.66[b]	8.63	12[c]	9.12	9.53[d] 8.42[f]	8.64	
				8.15[e] 8.5[g]				8.32[h]
$\epsilon_0^{\perp}$	6.82	6.87[b]	7.55	7.9[e]	8.45	9.02[d] 8.37[f]	8.64	

[a] The high-frequency dielectric constants used in the Lyddane-Sachs-Teller relationships were obtained from Table I in Ref. 17 for BeO; from W. L. Bond, J. Appl. Phys. **36**, 1674 (1965), for ZnO; and from T. M. Bieniewski and S. J. Czyzak, J. Opt. Soc. Am. **53**, 496 (1963), for CdS and ZnS.
[b] Table I in Ref. 17.
[c] Table IV in F. A. Kröger and H. J. G. Meyer, Physica **20**, 1149 (1954).
[d] D. Berlincourt, H. Jaffe, and L. R. Shiozawa, Phys. Rev. **129**, 1009 (1963).
[e] R. J. Collins and D. A. Kleinman, J. Phys. Chem. Solids **11**, 190 (1959).
[f] H. W. Verleur and A. S. Barker, Jr., Phys. Rev. **155**, 750 (1967).
[g] A. R. Hutson, Phys. Rev. **108**, 227 (1957).
[h] Cubic value from d.

cm^{-1} as the low-frequency E_2 mode. This line was not seen in our low-temperature spectra because of its $(n+1)$ intensity reduction and due to a lower signal-to-noise ratio resulting from crystal fluorescence.

We have found that the high-frequency E_2 mode in ZnS is coincident with the TO mode. This was verified by carefully studying the depolarization of this line at low temperatures. In Fig. 13 we show this result. With the normal gathering aperture there are two prominent lines in the $xy(E_2)$ spectrum, one at 356 cm^{-1} and one at 280 cm^{-1}. By reducing the aperture from ~f1.5 to ~f8 the intensity ratio of these two lines changed drastically, indicating that the apparent intensity of the 356-cm^{-1} line resulted from the high collection angles used in the observation, while the 280-cm^{-1} line, even though decreasing in intensity with decreasing collection angle, clearly shows a nonzero xy polarizability component and thus has E_2 character. Our ZnS results are summarized in Table II, where both the room-temperature and the low-temperature data are tabulated.

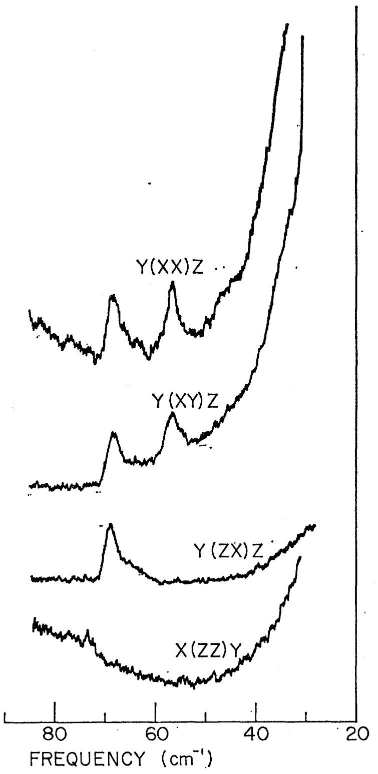

FIG. 12. Room-temperature Raman spectrum of the two low-frequency lines (68 and 55 cm^{-1}) of ZnS showing their depolarization characteristics.

From the polar phonon frequencies and the high-frequency dielectric constants, the static dielectric constants may be determined by use of the Lyddane-Sachs-Teller relationship. The derived values of the static dielectric constants for both the ordinary and extraordinary ray are listed in Table III.

B. Absolute Intensity Measurements

The intensity of a longitudinal phonon results from a deformation potential term and an electro-optic term.[7,11] By measuring the intensity of the transverse mode the magnitude of the deformation potential

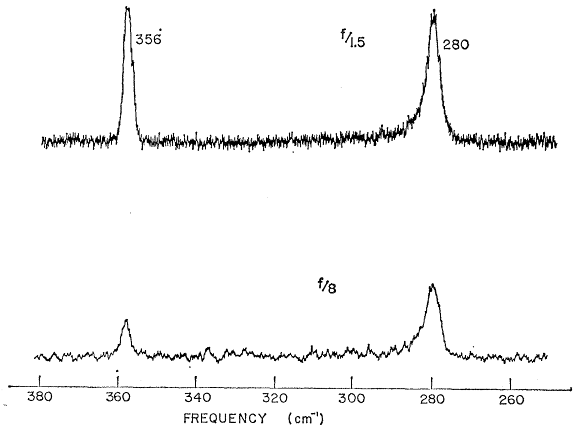

FIG. 13. $y(xy)z$ scattering from ZnS observed at two different gathering angles, demonstrating the E_2 character of the band at 280 cm^{-1}.

TABLE IV. Scattering efficiencies of polar phonons and calculated electro-optic coefficients of BeO, ZnO, and CdS.

	BeO			ZnO			CdS (25°K)		
Scattering efficiencies (10^{-8}/cm sr)	α_{xx}	α_{zz}	α_{xz}	α_{xx}	α_{zz}	α_{xz}	α_{xx}	α_{zz}	α_{xz}
TO	1.42	5.14	0.590	3.25	3.18	1.28	12.9	1.78	1.55
LO	0.703	1.75	0.221	0.00	5.17	0.418	31.2	15.8	8.04
Electro-optic coefficients (10^{-12} m/V)	Z_{31}	Z_{33}	Z_{15}	Z_{31}	Z_{33}	Z_{15}	Z_{31}	Z_{33}	Z_{15}
This work	1.5	2.6	1.3		3.1	1.3	7.0	4.1	4.8
	0.075	0.38	0.18	1.2	0.83	0.19	2.0	2.2	2.2
Literature values[a]	...	...	...	1.4	2.6	...	1.1	2.4	...

[a] Table IV of Ref. 24.

scattering term may be found. Using this value, electro-optic coefficients can be determined from absolute intensity measurements of the longitudinal phonon. We may rewrite Eqs. (5) and (6) in the form

$$S_l=\frac{\hbar\omega_l(n_l+1)L\Omega}{4\pi c^4}\left[\frac{1}{\omega_l}\left(\frac{S_t}{A}\right)^{1/2}-\frac{\omega_i{}^2\epsilon^2}{2}\left(\frac{1}{\epsilon}-\frac{1}{\epsilon^0}\right)^{1/2}Z_{ij}\right]^2, \quad (8)$$

where

$$A=\hbar(n_l+1)L\Omega/4\pi\omega_t c^4$$

and has been modified to be consistent with the geometry used in this investigation. Therefore, by measuring the absolute intensity for a given scattering length and solid angle electro-optic coefficients can be determined.

The three independent electro-optic coefficients for wurtzite are $Z_{13}=Z_{23}$, Z_{33} and $Z_{42}=Z_{51}$. Z_{13} and Z_{23} correspond to the xx and yy terms of the polarizability tensor with a polarization in the z direction; Z_{33} corresponds to the zz component polarized in the z direction, and Z_{42} and Z_{51} correspond to the zy and zx components with polarizations in y and x directions, respectively.

To obtain the Z_{15} or Z_{24} components of the electro-optic coefficients, $x(zx)y$ spectra were taken in which the E_1 TO and E_1 LO phonons polarized in the x direction could be observed. As the E_2 modes are not present in these spectra it was necessary to rotate the polarization of the incident beam with a half-wave plate to obtain an $x(yx)y$ spectrum which contained the E_2 secondary standard. The Z_{31} and Z_{32} electro-optic coefficients correspond to the xx component of the polarizability tensor, which is an A_1 phonon with a polarization in the z direction. To obtain the TO cross section $y(xx)\bar{y}$ scattering was used while $z(xx)\bar{z}$ was used to obtain the LO phonon intensity. Each of these spectra contained the E_2 secondary standard. The Z_{33} electro-optic coefficient may be found from the zz component of the polarizability tensor. The transverse mode was found from the $y(zz)\bar{y}$ spectrum and the longitudinal mode from the $\bar{x}(zz)\bar{x}$ spectrum. In both cases the polarization of the incident beam and of the analyzer was rotated by 90° to obtain the E_2 modes. The results of the absolute intensity measurements are listed in Table IV for each of the three crystals studied. Absolute intensity measurements were not made on ZnS as the high-frequency E_2 could not be separated from the TO phonon, making the TO phonon intensity measurement and the E_2 measurement extremely uncertain. Furthermore, the very low intensity of the low-frequency E_2 mode made it an unsuitable choice for an internal standard. In Table IV the values of the electro-optic coefficients, calculated from Eq. (7), are given. The frequencies used were those measured and reported in this paper, and the values used for the dielectric constant are those listed in Table III. We believe our values are accurate to within 20%.

In Table IV it is necessary to report two values for each electro-optic coefficient as the absolute sign of the deformation potential is not known. Furthermore, the sign of the electro-optic coefficient could not be determined from our measurements. Table IV also includes reported values of electro-optic coefficients as a comparison.[24] The literature values were direct electro-optic measurements made at constant strain and therefore give a high-frequency electro-optic coefficient and should very nearly correspond to the values obtained from Raman scattering. The excellent agreement between these values (when the proper signs are chosen) reflects the validity of Loudon's theory and furthermore indicates that valuable electro-optic coefficient measurements may be made directly by the Raman effect.

ACKNOWLEDGMENTS

We wish to thank Professor G. F. J. Garlick for a ZnS crystal and Dr. S. B. Austerman for the BeO crystal. Partial support from the National Science Foundation is gratefully acknowledged.

---

[24] I. P. Kaminow and E. H. Turner, Appl. Opt. 5, 1612 (1966).